Suzaku Wide-band All-sky Monitor (WAM) Observations of High Energy Transients

Kazutaka Yamaoka, [1] Satoshi Sugita, [1] Makoto S. Tashiro, [2] Yukikatsu Terada, [2] Yuji Urata, [2] Kaori Onda, [2] Akira Endo, [2] Natsuki Kodaka, [2] Kouichi Morigami, [2] Takako Sugasawara, [2] Wataru Iwakiri, [2] Yasushi Fukazawa, [3] Takuya Takahashi, [3] Takeshi Uehara, [3] Chie Kira, [3] Yoshitaka Hanabata, [3] Kazuo Makishima, [4] Kazuhiro Nakazawa, [4] Ryohei Miyawaki, [4] Teruaki Enoto, [4] Tadayuki Takahashi, [5] Motohide Kokubun, [5] Masanori Ohno, [5] Motoko Suzuki, [6] Soojing Hong, [7] Toru Tamagawa, [8] Yujin E. Nakagawa, [8] Makoto Yamauchi, [9] Eri Sonoda, [9] Ryoji Hara, [9] Yuki Tanaka, [9] Hidenori Hayashi, [9] Kenta Kohno, [9] Norisuke Ohmori, [9] Toshio Murakami, [10], Tsuneyoshi Kamae, [11] Hiroyasu Tajima, [11] and the Suzaku WAM team

[1]Department of Physics and Mathematics, Aoyama Gakuin University, Kanagawa, Japan
[2]Department of Physics, Saitama University, Saitama, Japan
[3]Department of Physics, Hiroshima University, Hiroshima, Japan
[4]Department of Physics, University of Tokyo, Tokyo, Japan
[5]Division of High Energy Astrophysics, ISAS/JAXA, Kanagawa, Japan
[6]ISS project team, ISAS/JAXA, Ibaraki, Japan
[7]College of Science and Technology, Nihon University, Tokyo, Japan
[8]Institute of Physical and Chemical Research (RIKEN), Saitama, Japan
[9]Department of Applied Physics, University of Miyazaki, Miyazaki,Japan
[10]Department of Physics, Kanazawa University, Kanazawa, Japan
[11]Stanford Linear Accelerator Center (SLAC), CA, USA
E-mail(KY): yamaoka@phys.aoyama.ac.jp

Abstract

The wide-band all-sky monitor (WAM) is the secondary function of large BGO shields of the Hard X-ray Detector (HXD) on board the Suzaku mission. Owing to its large geometrical area of 800 cm^2 per side and wide field of view, the WAM is very powerful to study soft gamma-ray transients in the energy range of 50–5000 keV. The main scientific objectives are gamma-ray bursts (GRB), soft gamma-ray repeaters (SGR), solar flares, and black-hole binaries. 449 GRBs, 78 SGRs, and 171 solar flares confirmed by other satellites were detected during the three-years operation (August 2005 to September 2008). The GRB detection rate is more than 140 per year, which shows one of the highest in current GRB missions. High quality spectra and light curves can be obtained for bright GRBs, which enable us to investigate the time variability and the time resolved spectroscopy even for the short duration GRBs. Furthermore, the WAM detected a large flare from the black-hole binary Cygnus X-1 corresponding to TeV gamma-ray detections with MAGIC telescope on September 2006. In this paper, we will review the results obtained from the WAM, and report on the current status of the WAM observations of these high energy transients.

Key words: gamma-ray burst, Suzaku, gamma-rays

1. Suzaku Wide-band All-sky Monitor(WAM)

The Suzaku is the fifth Japanese X-ray astronomical satellite which was launched on July 10th, 2005 (Mitsuda et al. 2007). It is flown into a near-Earth orbit with the altitude of 570 km and the inclination angle of 31 degrees. It carries three scientific instruments: X-ray spectrometer (XRS), X-ray imaging spectrometer (XIS), and hard X-ray detector (HXD; Takahashi et al. 2007, Kokubun et al. 2007). Currently two instruments (XIS and HXD) are operational well, covering a broad energy range of 0.3–600 keV.

The Suzaku wide-band all-sky monitor (WAM) is a subsystem of the HXD utilizing 20 lateral BGO anti-coincidence shields (Figure 1). The main purpose of the WAM is background rejection to the main detectors (Si PIN diodes and GSOs), but owing to its large geometrical area of 800 cm^2 and its large field of view of a half sky, it can be an ideal gamma-ray burst detector with an energy range of 50–5000 keV. Furthermore, the on-axis effective area per one wall (of the four walls) is about

400 cm^2 at 1 MeV (Figure 2), which is much larger than those of other GRB missions. Hence, the WAM is expected to clarify the origin of radiation mechanisms of the GRB prompt MeV gamma-ray emissions with a high sensitivity. The WAM characteristics are shown in Table 1

In this paper, we present the current status of the Suzaku WAM over initial three years, focusing on observations of GRBs and hard X-ray sources related with the MAXI science. Details of design and its in-orbit performance of the Suzaku WAM are described in Yamaoka et al. (2009).

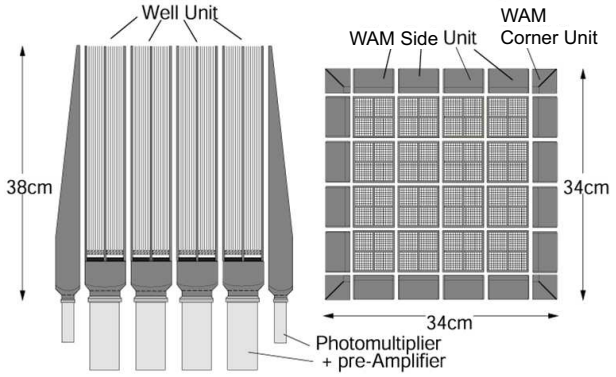

Fig. 1. Schematic view of the Hard X-ray Detector. Left panel: Cross-sectional view. Right panel: Top view. The WAM is a subsystem of the HXD which consists of the surrounding 20 BGO anti-coincidence shields.

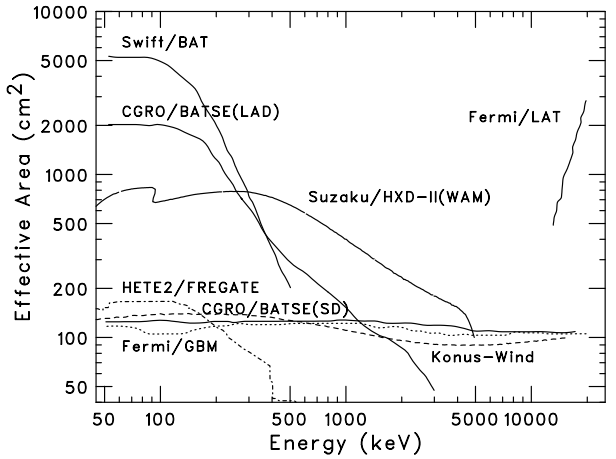

Fig. 2. On-axis effective area of the Suzaku WAM in comparison with previous and current GRB detectors. The Suzaku WAM has a very large effective area ∼400 cm^2 in the MeV range.

2. Current Status of Suzaku WAM

The WAM activation was completed on August 17, 2005. Since then, all the 20 WAM sensors have been working very well. There are also no problems in the

Table 1. Characteristics of the Suzaku wide-band all-sky monitor.

Sensors	20 BGO crystals + PMT
Number of detectors	4 (referred to as WAM 0–3)
Energy range	50–5000 keV (55 channels)
Geometrical area	800 cm^2 per side
Effective area	400 cm^2 per side @ 1 MeV
Energy resolution	$\sim$ 30% @ 662 keV
Field of view	$\sim 2\ \pi$
Time resolution	1/64s during 64 seconds (BST data)$*$; every 1s (TRN data)
Telemetry rate	5 kbps
Response to GRBs	within a day (no alerts)
GRB localization capability	5–10 degrees (WAM alone), <1 degree (IPN)

$*$ Since Mar. 20, 2006. 1/32 s during 128 seconds before this date.

WAM electronics including the data readout and GRB trigger system. Table 2 shows statistics of the WAM events from August 2005 to September 2008. 449 GRBs were confirmed by other satellites, while 298 GRB-like events were not confirmed and classified as possible GRBs. It means that the WAM has been detecting more than 140 GRBs per year. We have released 74 GCN circulars about the WAM spectral parameters and Inter-Planetary Network (IPN; IPN3 web site: http://ssl.berkeley.edu/ipn3/index.html) localization. The WAM sensitivity for 1-sec is estimated at ∼0.7 photons cm^{-2} s^{-1} in the 50−300 keV range. The funding for the Suzaku operation is approved for at least two more years, so the WAM will continue to detect GRBs at the same rate unless it does not work.

The energy-scale calibration is performed using the 511 keV line from surrounding activated materials on the satellite. We monitor the gain of all the units at once a day. The WAM absolute flux calibration is performed using GRBs which was simultaneously detected by Swift-BAT and Konus-Wind (Yamaoka et al. 2009 and Sakamoto et al. 2009). The current flux uncertainties above 120 keV are estimated at ∼30 % except for the XRS directions. Uncertainties for lower energy than 120 keV are at more than 40 %, probably due to additional absorptions from the satellite. Similar results have been obtained using Crab Nebula with the Earth-occultation technique. Further refinement of calibrations and study of GRB localization by the WAM alone are still under way. Absolute timing has been verified by measuring the time delay for position well-determined GRBs with IPN. Thus, the Suzaku WAM has been involved into the third IPNs and has played an important role as one of detectors in the low-Earth orbit.

Table 2. Statistics of the WAM events, through August 2005 to September 2008.

Category	Number (Trigger)
Confirmed GRBs	449 (274)
Swift/BAT	85 (44)
Fermi/GBM	27 (15)
INTEGRAL/IBIS	6
AGILE/superAGILE	6
Konus-Wind	364
Possible GRBs	298 (139)
Soft Gamma-ray Repeaters	78 (5)
Solar flares	171 (28)

3. WAM Observations of Gamma-ray Bursts

3.1. GRB Light Curves and Energy Spectra

The WAM can get the fine-time resolution light curve with 1/32 or 1/64 sec (BST data) in case a GRB trigger the WAM. We also continuously get the energy spectrum with 1-sec time resolution (TRN data). Figure 3 shows the light curve of the short-duration GRB 060317 in the four energy bands with 1/32 sec resolution. This GRB has a peak flux of 41±4 photons s^{-1} cm^{-2} in the 50-5000 keV range, and a very hard spectrum with $E_{\rm peak}$ ∼2 MeV (Ohno et al. 2008). Ohno et al. (2008) also estimated a lag between the 50–110 keV band and other three bands (110–240 keV, 240–520 keV, and 520–5000 keV), and found that all were consistent with zero, indicating that this GRB indeed belongs to the short-burst category. Thus, the WAM can produce high quality data for variability studies even in the highest energy range above 520 keV owing to its large effective area. The light curve data for confirmed GRBs are available at the web site: http://www.astro.isas.jaxa.jp/suzaku/HXD-WAM/WAM-GRB/

The T90 duration distribution for triggered bursts is shown in Figure 4. We have plotted it for confirmed GRBs and possible GRBs. The T90 duration was calculated as the time interval starting after 5% and ending after 95% of the counts in the 50–5000 keV range. The distribution of the BATSE sample in the 4th revised catalog (Paciesas et al. 1999) is also shown for comparison. We clearly observe a bimodal distribution for confirmed GRBs which peaks at 0.2 sec and 10 sec. This is almost consistent with the BATSE sample, but is quite different from the Swift distribution, which has relatively few short-duration GRBs (<2 sec) (Sakamoto et al. 2008).

An important feature of the WAM is its large effective area in the MeV range. Figure 5 shows time-averaged spectra in raw detector counts for six bright GRBs which were localized by the IPN. This sample includes two short GRBs: GRB 051103 and GRB 060317. All the

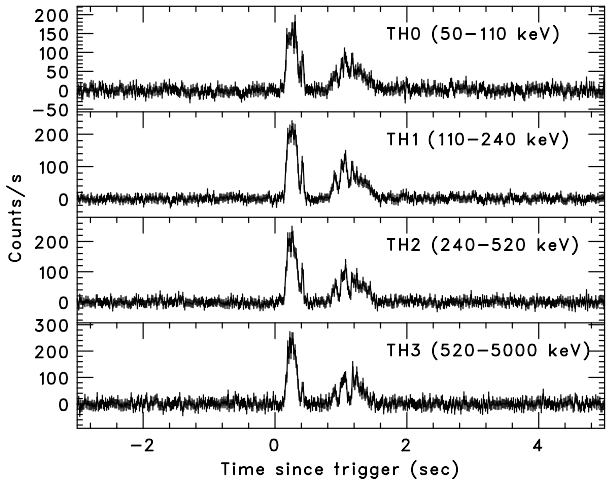

Fig. 3. Example of the bright short GRB 060317 in the four energy bands. High quality light curve can be obtained even in the highest energy band (>520 keV).

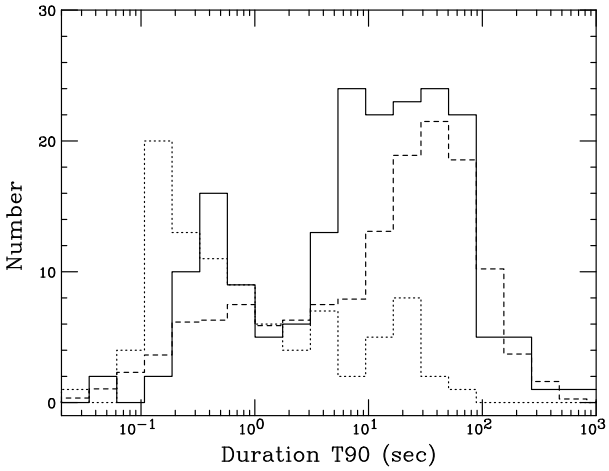

Fig. 4. T90 duration distributions of the WAM GRBs. Confirmed and possible GRBs are shown separately as solid and dotted lines, respectively. They are also compared with BATSE GRB sample (dashed line) with an arbitrary normalization.

bursts (even the short bursts) show clear signals above 1 MeV. High quality spectra can be obtained up to $\sim$ 5 MeV. This capability is a very powerful tool in determining the high energy photon index β and studying the connection between the low energy component, presumably due to synchrotron emission, and the poorly understood high energy component (> MeV) detected by EGRET/TASC (Gonzalez et al. 2002), which might be detected by Fermi and AGILE.

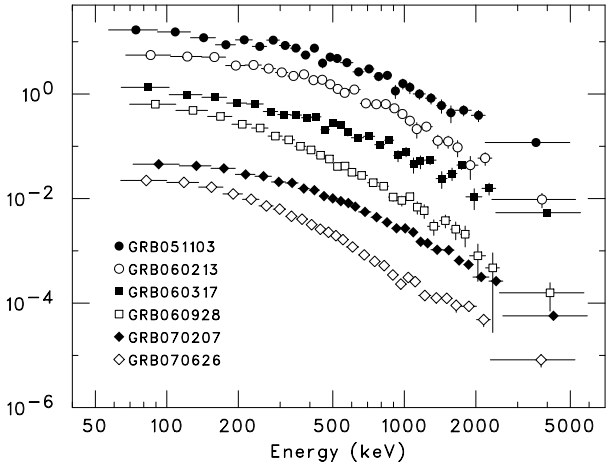

Fig. 5. Example of WAM count spectra for six bright GRBs. GRB 051103 and GRB 060317 are classified as short-duration bursts.

3.2. Joint Swift/BAT and Suzaku/WAM Spectral Analysis

Broadband spectral measurements of the GRB prompt emissions are important in understanding the GRB radiation mechanisms. In addition, several correlations among GRB spectral parameters such as peak energies ($E_{\rm peak}$) have been proposed and discussed. Some of them are used for redshift indicators and constraints on cosmological constants. Rapid localizations by Swift has enabled us to determine redshifts for many GRBS, however, only 14% of the Swift GRBs have $E_{\rm peak}$ due to the limited energy range of BAT (15−150 keV). Figure 6 shows an example of Swift-BAT and Suzaku-WAM $_{\nu}F_{\nu}$ spectra of the three Swift GRBs. The peaks of the spectra ($E_{\rm peak}$) is clearly visible in the 50 keV to 1 MeV range, so a combination of Swift/BAT (15−150 keV) and Suzaku/WAM (50−5000 keV) can be very powerful tool to determine GRB spectral parameters.

Since 2006 August, we are going to proceed joint spectral analysis project between Swift/BAT and Suzaku/WAM (Krimm et al. 2009). We have paid careful attention for the cross-calibration issue and analysis methods. 85 GRBs (44 WAM triggers and 41 untriggers) were detected by both instruments till September 2008, and 32 GRBs have known redshifts in their range of 0.089(GRB 060505) to 6.295 (GRB 050904; Sugita et al. 2009). All the bursts were jointly analyzed, and $E_{\rm peak}$ was determined for 51 GRBs. Figure 7 shows updated $E_{\rm p,i}$-$E_{\rm iso}$ correlations, so-called Amati relations, for BAT-WAM GRBs. Long GRBs satisfied with this relations within statistical errors, but there might be some bias to larger $E_{\rm peak}$. On the other hand, all the six short GRBs (GRB 051221A, 060801, 061006, 061210, 070714B and 071227) and sub-luminous GRB 060505 are outliers in the Amati relation. $E_{\rm peak} - L_{\gamma}$ (Ghirlanda relation; Ghirlanda et al. 2004) and $E_{\rm peak} - L_{\rm p}$ (Yonetoku relation; Yonetoku et al. 2004) are still under investigation.

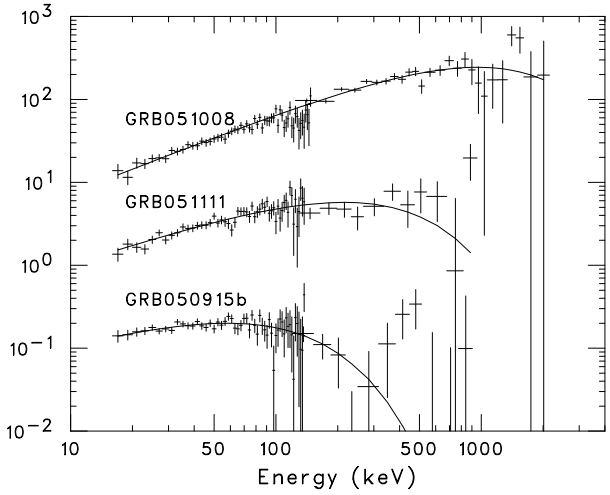

Fig. 6. Unfolded $_{\nu}F_{\nu}$ energy spectra of the three Swift GRBs (GRB 050915B, GRB 051111 and GRB 051008). A combination of Swift/BAT and Suzaku/WAM is very powerful to determine the peak energy ($E_{\rm peak}$) in the range of 50–1000 keV.

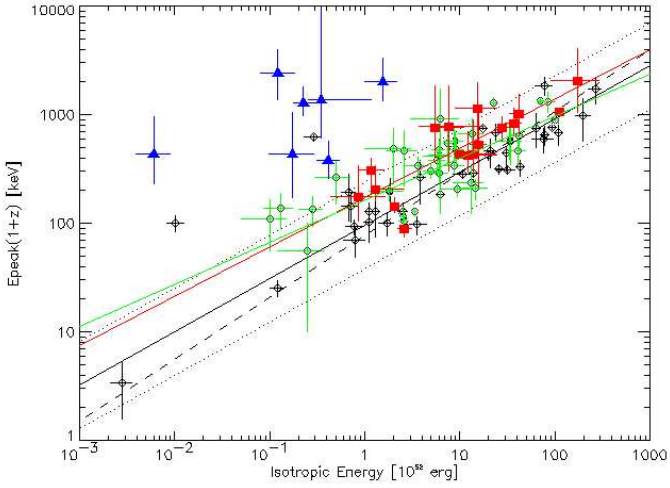

Fig. 7. Correlation between peak energy ($E_{\rm peak}$) and isotropic radiated energies ($E_{\rm iso}$) (Amati 2006). Short and log bursts are shown by triangles and squares, respectively.

Both Swift-BAT and Suzaku-WAM have a very large

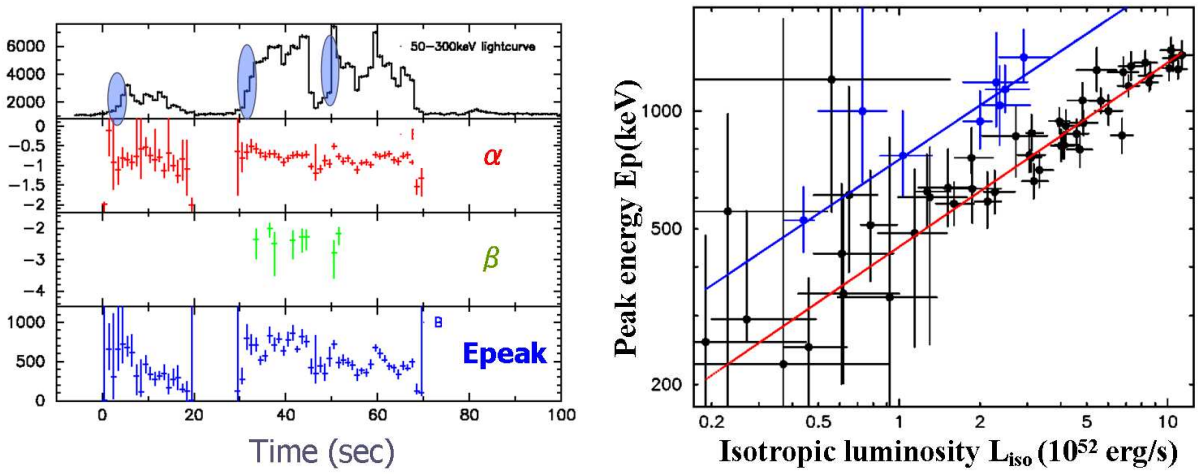

Fig. 8. Left:Time evolution the burst intensity and the spectral parameters of GRB 061007. The $E_{\rm peak}$ is variable with time. Right: Correlation between isotropic luminosity $L_{\rm iso}$ (10^{52} erg s^{-1}) and peak energy $E_{\rm peak}$ (keV) for individual 1-sec segments. Clear correlations are found except for the pulse rising phase (hatched region of left panel of the Figure).

effective area, so it is suitable for time-resolved spectroscopy of bright GRBs and verification of correlations between $E_{\rm peak}$ and $L_{\rm iso}$ (Yonetoku et al. 2004, and Liang et al. 2004). Long-duration GRB 061007 is the most brightest burst in the BAT-WAM sample with 1-sec peak flux of 14 photons cm^{-2} s^{-1} in the 100−1000 keV range (Ohno et al. 2009). We performed a joint spectral fitting with the Band function (Band et al. 2002) every 1 sec (minimum time resolution of the TRN data). Left panel of Figure 8 shows the time evolution of source intensity and spectral parameters (peak energy $E_{\rm peak}$, photon index α below $E_{\rm peak}$, photon index β above $E_{\rm peak}$). The burst shows typical hard-to-soft evolutions, and the $E_{\rm peak}$ is variable with the burst intensity. Right panel of Figure 8 shows correlation between $E_{\rm peak}$ and $L_{\rm iso}$ for 1-sec segment. A clear correlation between these two parameters is found as $E_{\rm peak} \propto L_{\rm iso}^{0.46\pm0.03}$ except for the initial rising phase of the burst pulse (see hatched regions of left panel of Figure 8). This relation is consistent with expected one from synchrotron shock model ($E_{\rm peak} \propto L_{\rm iso}^{1/2}$). Another possible correlation might be seen in the rising phase, suggesting that its origin is physically different (*e.x.* acceleration process) or it has different physical parameters (bulk Lorentz factor or/and shock radius) from other phases.

4. WAM Observations of Hard X-ray Sources

Bright hard X-ray sources with an intensity of ∼1 Crab can be monitored by the WAM using the Earth occultation methods developed by the CGRO/BATSE team (Harmon et al. 2002). This method measures the step in the flux contribution when the source rises above and sets below the Earth horizon. The WAM is an ideal detector for this purpose because its field of view is not limited. The current all-sky monitors are the RXTE/ASM, which operates in the 1.5–12 keV band and the Swift/BAT in the 15–50 keV range, so the WAM can provide unique opportunities to monitor sources in the range above 50 keV to fill the high energy end.

We have searched for the contributions from known sources expected at specific times based on the Suzaku orbital elements. Figure 9 shows the Earth-occultation step for the Crab Nebula. This was obtained by summing 16 orbits with the same satellite attitude. In addition to bright X-ray binaries such as Cygnus X-1 and GRS 1915+105, weak sources such as the radio galaxy Cen-A and the Seyfert galaxy NGC 4151 have been detected with the WAM. The sensitivity is estimated at about 300 mCrab and 30 mCrab in the 50–300 keV range for integrations of one-day and two-years, respectively.

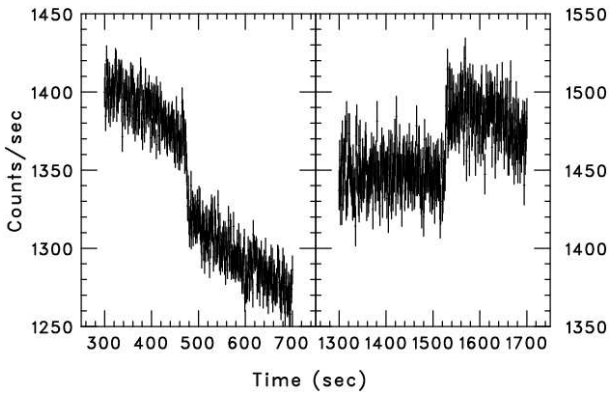

Fig. 9. Earth occultation step for the Crab Nebula observed by WAM 0 in the 50-300 keV range.

Figure 10 shows preliminary results of long-term light curve of the black hole binary Cygnus X-1 in the 100-300 keV range over two years. It is compared with publicly available data taken by Swift/BAT and RXTE/ASM. The WAM light curve is resemble with Two important events were seen from this light curve: 1) a possible state transition from the low/hard state to the high/soft state occurred on April 2006 (decrease of hard X-rays), and 2) a hard X-ray flare was observed in correspondence with MAGIC detection of very high energy gamma-rays on September 2006 (Albert et al. 2007). These data will be publicly available at the WAM web site. Details of the Earth occultation results are described in Kira et al. (2008).

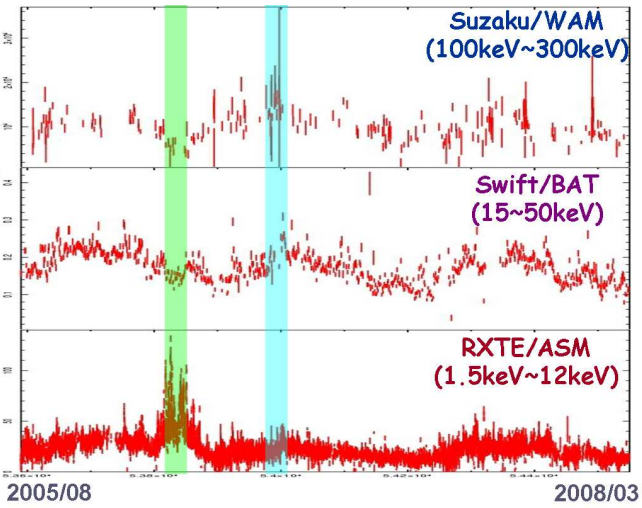

Fig. 10. Long-term Suzaku-WAM light curve of the black hole candidate Cygnus X-1 in comparison with Swift-BAT(15-50 keV) and RXTE/ASM (1.5-12 keV). We can see 1)possible state transition from the low/hard to the high/soft state on April 2006 and 2)a hard X-ray flare which corresponds to the MAGIC VHE gamma-ray detection on September 2006 (Albert et al. 2007).

5. Summary

We have presented current status of the Suzaku Wide-band All-sky Monitor (WAM) utilizing the anti-coincidence shield of the Hard X-ray Detector (HXD). The 20 BGO sensors and their electronics have been operating nominally since Suzaku launch. The WAM has been detecting 140 GRBs per year. and succeeded in detecting hard X-ray sources using the Earth occultation method. The different energy coverage of MAXI (0.3–30 keV) and Suzaku-WAM (50–5000 keV) will be complementary for both science.

References

Albert J. et al. 2007 ApJ., 665, L51
Amati L. 2006 MNRAS., 372, 233
Band D. et al. 1993 ApJ., 413, 281
Ghirlanda G. et al. 2002 A&A., 393, 409
Gonzalez M.M. et al. 2002 Nature, 424, 749
Harmon B.A. et al. 2002 ApJS., 138, 149
Kira C. et al. 2008, in this volume
Kokubun M. et al. 2007 PASJ., 59, S53
Krimm H. et al. 2009 ApJ., in preparation
Liang et al. 2004 ApJ., 606, 29
Mitsuda K. et al. 2007 PASJ., 59, S1
Ohno M. et al. 2008 PASJ., 60, S361
Ohno M. et al. 2009 PASJ., 62, accepted
Paciesas W.S. et al. 1999 ApJS., 122, 465
Sakamoto T. et al. 2008 ApJS., 175, 179
Sakamoto T. et al. 2009 PASJ., in preparation
Sugita S. et al. 2009 PASJ., submitted
Takahashi T. et al. 2007 PASJ., 59, S35
Yamaoka K. et al. 2009 accepted for PASJ. third Suzaku special issue
Yonetoku D. et al. 2004 ApJ., 609, 935